UNIVERSITY OF CALIFORNIA SAN DIEGO

Characterizing the Role of LMPTP in Adipogenesis & Discovery of New LMPTP Inhibitors

A thesis submitted in satisfaction of the requirements
for the degree Master of Science

in

Biology

by

Zachary James Holmes

Committee in charge:

Professor Stephanie Stanford, Chair
Professor Enfu Hui, Co-chair
Professor Katherine Petrie

2021

The thesis of Zachary James Holmes is approved, and it is acceptable in quality and form for publication on microfilm and electronically.

University of California San Diego

2021

DEDICATION

In recognition of Dr. Stephanie Stanford for her role in supporting my research, training me as a scientist, and for the much-appreciated mentorship.

In recognition of Dr. Nunzio Bottini for setting a strong example of what it means to be a scientist of upstanding quality.

In recognition of Michael Diaz whose efforts were essential for laying the groundwork for my research, and for training me in virtually everything I know inside the lab.

In recognition of my parents and close friends who helped me through all the challenging times. I am beyond grateful for their love and support which allowed me to see my degree(s) to completion.

TABLE OF CONTENTS

LIST OF ABBREVIATIONS

ACP1 – Acid phosphatase 1

ANOVA – Analysis of variance

ASO – Antisense oligonucleotide

BCS – Bovine calf serum

BSA – Bovine serum albumin

CEBP – CCAAT-enhancer binding protein

CST – Cell Signaling Technologies

DIO – Diet-induced obese

Dex – Dexamethasone

DMEM – Dulbecco's modified eagle medium

DMSO – Dimethyl sulfoxide

DPC – Days post-confluence

EMEM – Eagle's minimum essential medium

FBS – Fetal bovine serum

Fructose 1,6BP – Fructose-1,6-bisphosphate

H&E – Hematoxylin and eosin

HFD – High fat diet

HK2 – Hexokinase 2

IBMX – 3-isobutyl-1-methylxanthine

IDT – Integrated DNA Technologies

IP – Immunoprecipitation

IPTG – Isopropyl β-d-1-thiogalactopyranoside

JNK – C-Jun N-terminal Kinase

KO – knockout

LMPTP – Low molecular weight protein tyrosine phosphatase

MAPK – Mitogen-activated protein kinase

mETC – Mitochondrial electron transport chain

PCA – Principal component analysis

PDGFRα – Platelet-derived growth factor receptor alpha

PEP – Phosphoenolpyruvate

pNPP – Para-nitrophenyl phosphate

PPARγ – Peroxisome proliferator-activated receptor gamma

PPP – Pentose phosphate pathway

PTP – Protein tyrosine phosphatase

RBC – Red blood cells

RTK – Receptor tyrosine kinase

SDS-PAGE – Sodium dodecyl sulfate-polyacrylamide gel electrophoresis

SubQ – Subcutaneous

TBST – Tris buffered saline with Tween

TCEP – Tris(2-carboxyethyl)phosphine

WAT – White adipose tissue

WT – Wildtype

Y/A – Tyrosine to alanine mutant

LIST OF FIGURES

LIST OF SCHEMES

LIST OF TABLES

ACKNOWLEDGEMENTS

Figures 1, 3, and 4 are coauthored by Zachary Holmes and Michael Diaz. Zachary Holmes is the secondary author for figures these figures.

Figure 2 is coauthored by Zachary Holmes, Michael Diaz, Matthew Bliss, and Vida Zhang. All authors contributed equally to this figure.

Figures 5 and 10 are coauthored by Zachary Holmes and Michael Diaz. Zachary Holmes is the primary author for these figures.

Figure 6 is coauthored by Zachary Holmes, Meghan Collins, and Michael Diaz. Zachary Holmes and Meghan Collins are the primary authors of this figure and contributed equally.

Figure 7 is coauthored by Zachary Holmes and Meghan Collins. Both authors contributed equally to this figure.

ABSTRACT OF THE THESIS

Characterizing the Role of LMPTP in Adipogenesis &
Discovery of New LMPTP Inhibitors

by

Zachary Holmes

Master of Science in Biology

University of California San Diego, 2021

Professor Stephanie Stanford, Chair

Professor Enfu Hui, Co-chair

Obesity is an ongoing epidemic and major contributor to the development of Type 2 diabetes. Multiple studies into the low molecular weight protein tyrosine phosphatase (LMPTP) have provided evidence for its role in the severity of obesity-related illnesses. Our lab previously reported that LMPTP drives insulin resistance in obesity by negatively regulating liver insulin signaling, and that inhibition of LMPTP relieves the severity of obesity-induced diabetes in mice. LMPTP is highly expressed in adipose tissue, and here, we report a characterization of the role of LMPTP in adipocyte differentiation. Using conditional knockout mice and *in vitro* adipogenesis assays, we found that a loss of LMPTP activity in preadipocytes reduces adipocyte differentiation. Inhibition of LMPTP during adipogenesis blocks expression of the pro-adipogenic transcription factor peroxisome proliferator-activated receptor gamma (PPARγ) and its downstream target genes. Interestingly, LMPTP inhibition enhances basal platelet-derived growth factor receptor alpha (PDGFRα) signaling, resulting in increased activation of p38 & c-Jun-N-terminal kinase (JNK), and increased inhibitory phosphorylation of PPARγ. Metabolomic analysis of differentiating 3T3-L1 preadipocytes suggests that LMPTP inhibition results in a phenotype closer to proliferation than differentiation, as evidenced by enhanced mitochondrial respiration and nucleotide synthesis. Finally, we characterized a new series of LMPTP inhibitors. We describe the role of Tyr131 of LMPTP in mediating inhibition and demonstrate that an inhibitor from this series is viable for cell-based assays. In summary, we propose a novel mechanism for the role of LMPTP in adipocyte differentiation while additionally providing new insight into possible strategies to target LMPTP for inhibition.

INTRODUCTION

The first step to treating or curing diseases is to understand the underlying pathologies associated with their development. Understanding these pathologies requires examination of everything from the genetic background of highly susceptible individuals to the cell signaling pathways that lead to diseases, and everything in between. One set of diseases that are increasing in relevance are obesity-related illnesses, as developed nations around the world are experiencing an increase in the rate of obesity in their populations. As of 2017-2018, between a third and half of US adults were characterized as obese (Hales et al., 2020), and that number continues to rise to this day.

An obesity-related illness that warrants further investigation is type II diabetes (T2D). Patients with T2D exhibit a poor response to insulin, a condition known as insulin resistance (Chooi et al., 2019). The pathology of T2D is tied directly to the development of insulin resistance, and as such, understanding the mechanisms through which insulin signaling is regulated in cells is of great concern to scientists and patients suffering from the disease. One proposed method for combating insulin resistance is to target the protein tyrosine phosphatases (PTP) that negatively regulate insulin receptor (IR) signaling for inhibition (Musi & Goodyear, 2006). One example of this is PTP1B, a known negative regulator of insulin signaling which acts by dephosphorylating activation residues of the IR (Johnson et al., 2002). Unfortunately, structural features of this class of enzymes — namely a small highly charged and well-conserved active site — make targeting these enzymes with any notable specificity very difficult (Stanford & Bottini, 2017).

The low molecular weight protein tyrosine phosphatase (LMPTP) is a small (18 kDa) ubiquitously expressed PTP that is encoded by the acid phosphatase I (*ACP1*) gene (Wo et al.,

1992). LMPTP and the PTP SSU72 are the lone members of the class II subfamily of PTPs, making them unique relative to the vast majority of PTPs (Alonso et al., 2016). Research on the genetic profile of LMPTP in humans suggests that *ACP1* expression is associated with clinical variability in obesity-related illnesses (Bottini et al., 1990). Early studies on the subject demonstrate that *ACP1* genotypes encoding for low LMPTP enzymatic activity protect against hyperglycemia and dyslipidemia in obese individuals (Lucarini et al., 1997; Bottini et al., 2002). Previously, LMPTP has been reported to be a negative regulator of receptor tyrosine kinase (RTK) signaling (Caselli et al., 2016). Specifically, LMPTP has been shown to be a negative regulator of insulin signaling by interacting directly with the IR (Chiarugi et al., 1997). Our lab has also previously demonstrated that LMPTP knockout (KO) and inhibition of LMPTP in diet-induced obese (DIO) mice enhances insulin signaling in a liver-specific manner (Stanford et al., 2017). Similarly, LMPTP knockdown using antisense oligonucleotides (ASO) has been shown to decrease insulin resistance in DIO mice while enhancing liver IR phosphorylation (Pandey et al., 2007). These results provide substantial evidence in addition to the genetic studies to suggest that LMPTP plays a key role in obesity-associated insulin resistance.

In addition to its role in liver IR signaling, LMPTP has also been reported to regulate another RTK, the platelet-derived growth factor receptor (PDGFR). NIH-3T3 fibroblasts overexpressing LMPTP were shown to have reduced proliferative response to fetal bovine serum (FBS) or PDGF (Berti et al., 1994). Similarly, a study demonstrated that overexpression of the catalytically inactive LMPTP C12S mutant leads to enhanced PDGF-induced tyrosine phosphorylation of the RTK (Chiarugi et al., 2002). Interestingly, studies have shown that PDGFR signaling is inhibitory for white adipose tissue (WAT) development (Artemenko et al., 2005). PDGF has been shown to inhibit adipocyte differentiation — a process referred to here as

adipogenesis — in 3T3-L1 preadipocytes. Additionally, primary preadipocytes overexpressing the constitutively active PDGFRα D842V mutant exhibit substantially impaired adipogenesis, as well as a significant reduction in expression of the peroxisome proliferator-activated receptor gamma (PPARγ) (Accili & Taylor, 1991), a protein that serves as the primary transcription factor regulating white adipocyte differentiation.

Since LMPTP is expressed in adipose tissue, yet its role has not been clearly defined, we sought to better understand the role of LMPTP in adipocyte biology. Using a combination of adipocyte-specific LMPTP KO, *in vitro* adipogenesis assays, cellular signaling, and metabolomic analyses, we propose a mechanism for the role of LMPTP in promoting subcutaneous (SubQ) adipocyte differentiation. We propose that LMPTP acts on the PDGFRα to promote adipogenesis and simultaneously shift the metabolic profile of preadipocytes to accommodate their differentiation.

Finally, in addition to our exploration of the biological role of LMPTP in adipocytes, we also sought to characterize a new series of LMPTP inhibitors. These new inhibitors display significantly enhanced potency compared to our previously utilized inhibitors while still maintaining strong selectivity for LMPTP. To characterize the utility of these inhibitors, we described the importance of Tyr131 and Tyr132 of LMPTP in facilitating inhibition by compounds in this screening, and we also demonstrated that Compound 6g from this screening is viable for cell-based assays.

MATERIALS & METHODS

Antibodies & Other Reagents

LMPTP inhibitor Compound 23 was generated as described in (Stanford et al., 2017). LMPTP inhibitors Compound 5d and 6g were generated as described in (Stanford & Diaz et al., 2021) Antisense oligonucleotides (ASO) were purchased from Gene Tools, LLC. AdipoRed lipid stain was purchased from Lonza. 10X Cell Lysis Buffer was purchased from Cell Signaling Technology (CST). Descriptions of the antibodies used in this study are provided in the tables below. All primers used for qPCR were purchased from MilliporeSigma. Primers used for LMPTP mutagenesis were purchased from Integrated DNA Technologies (IDT) (Table 2). Unless otherwise stated, other chemicals and reagents were purchased from Sigma-Aldrich.

Table 1: Antibodies used in this study

Antibody (Product/Clone #)	Vendor	Dilution
PDGFRα (D1E1E)	CST	1:1000
PDGFRα/β pTyr849/857 (C43E9)	CST	1:1000
SAPK/JNK pThr183/Tyr185 (81E11)	CST	1:1000
p38 MAPK pThr180/Tyr182 (D3F9)	CST	1:1000
GAPDH (D16H11)	CST	1:1000
PPARγ pSer82/112 (PA5-36762)	ThermoFisher	1:1000
PPARγ (81B8)	CST	1:1000
AKT pThr308 (244F9)	CST	1:1000
pan-AKT (C67E7)	CST	1:1000
ECL anti-Rabbit IgG (95017-556)	GE Healthcare	1:3000

Mice

Animal experiments were performed according to the guidelines and protocols set forth & approved by the La Jolla Institute for Allergy & Immunology (#AP126-NB3) and the University of California San Diego (S16098). B6 mice were purchased from Jackson Laboratory (JAX#000664). Generation of *Acp1*-floxed mice carrying the Cre transgene expressed under the adiponectin (Adipoq) promoter was described in (Stanford et al., 2017). To generate DIO mice, male littermate *Acp1*-floxed Cre^+ and Cre^- mice were fed high-fat diet (HFD) chow containing 60 kcal % fat for 12 months starting at age 4-8 weeks.

Assessment of Subcutaneous Adipocyte Size

Isolated subcutaneous (SubQ) fat pads from male DIO *adipoq*-Cre^+ (LMPTP KO) & Cre^- (WT) littermate mice were fixed in formalin for 24 hours, processed, and embedded in paraffin, cut and stained with hematoxylin and eosin (H&E) according to standard protocols. Cell sizes were assessed using ImageJ.

Isolation of Primary Preadipocytes

Primary mouse wildtype (WT) and LMPTP knockout (KO) preadipocytes were isolated from SubQ fat pads by digestion in Hank's Balanced Salt Solution with 3% FBS, 1 mM CaCl2, 1 mM MgCl2, 10 mg/mL Collagenase II, and 2.4 U/mL Dispase II for 30 minutes. Digests were filtered through a 40 μm nylon cell strainer and centrifuged at 350 x g for 5 minutes. Red blood cells (RBC) were lysed using RBC Lysis Buffer from CST, and digests were further resuspended and centrifuged. The remaining preadipocytes were plated and cultured in Dulbecco's Modified Eagle Medium (DMEM)/F12 media containing 10% fetal bovine serum (FBS) with 100 U/mL

penicillin & 100 µg/mL streptomycin for the duration of the adipogenesis assay. Cells were differentiated as described below.

Adipogenesis/Differentiation Assay

3T3-L1 preadipocytes were cultured in DMEM supplemented with 10% bovine calf serum (BCS), 100 U/mL penicillin and 100 µg/mL streptomycin. Cells were seeded in six-well plates and grown to confluence. Undifferentiated cells were kept in BCS-containing media for the duration of the assay, and the media was changed every two days. Differentiated cells were treated with BCS-containing media until two days post confluence, at which point, the media was replaced with DMEM supplemented with 10 % FBS, 100 U/mL penicillin and 100 µg/mL streptomycin (FBS/DMEM). At two days post confluence, differentiated cells were stimulated with 170 nM insulin, 1 µM dexamethasone (Dex) and 0.52 mM 3-isobutyl-1-methylxanthine (IBMX). After two days, media was exchanged with FBS/DMEM containing 170 nM insulin. After two days of insulin-only stimulation, cells were grown in FBS/DMEM for the remainder of the assay until 10 days post-confluence.

For assays involving LMPTP inhibition, cells were treated with 0.1% dimethyl sulfoxide (DMSO) or 10 µM Compound 23 starting on the day of confluence, and every two days subsequently. For assays involving LMPTP knockdown, cells were treated with 10 µM non-targeting ASOs or LMPTP-targeting ASOs starting on the day of confluence, and on days two and four post-confluence. Adipogenesis was quantified by addition of AdipoRed lipid stain according to the manufacturer's instruction (Lonza). Accumulation of fat droplets was assessed by fluorescence, measured using a Tecan plate reader with excitation and emission at 485 nm and 572 nm respectively.

Quantitative Real-time PCR (qPCR)

For qPCR analysis, cells were lysed in RLT buffer (Qiagen) supplemented with 1% β-mercaptoethanol. Lysates were collected and RNA was isolated using RNeasy Micro Kits according to manufacturer instructions. RNA concentrations were measured using a NanoDrop before proceeding. cDNA synthesis was performed using the SuperScript III Kit according to manufacturer's instructions (Invitrogen) using the BioRad S1000 Thermal Cycler. cDNA was subsequently diluted 1:5 with RNase free water. Samples were prepared using 0.5 μM primers, RT SYBR Green qPCR reagent, RNase free water, and cDNA according to manufacturer's instructions. Gene expression was normalized to the housekeeping gene *Polr2a*.

Western blotting & PDGFRα Immunoprecipitation

For Immunoprecipitation and Western blot analysis, cells were first lysed in 1x Cell Lysis Buffer (CST) supplemented with 1 mM phenylmethylsulfonyl fluoride (PMSF). Lysates were incubated at 4°C for 10 minutes before collection and processing. The lysates were then sonicated at 4°C for 15 intervals of 10-15 seconds before clearing insoluble fractions by 4°C centrifugation. Protein quantification was assessed by Pierce BCA Protein Assay Kit (Thermo Scientific) before performing immunoprecipitation and/or sodium dodecyl sulfate-polyacrylamide gel electrophoresis (SDS-PAGE).

For PDGFRα immunoprecipitation, lysates were incubated for 2 hours at 4°C with anti-PDGFRα (D1E1E) antibody. Next, lysates were incubated for 1 hour at 4°C with PG Sepharose antibody-binding beads (VWR). For Western blot analysis, protein lysates or immunoprecipitation beads were loaded onto pre-cast Novex Tris-Glycine gels (Thermo Scientific) and ran at 120V. Proteins were transferred onto 0.45 μm nitrocellulose membranes

and blocked in a 5% bovine serum albumin (BSA) in tris buffered saline with tween (TBST) solution. Membranes were incubated with primary antibodies in a 5% BSA/TBST solution for 1-2 hours at room temperature or overnight at 4°C, washed three times with TBST, incubated with secondary antibody in a 5% non-fat powdered milk in TBST solution, and finally washed three times with TBST. Membranes were then treated with Crescendo Western HRP substrate (Millipore Sigma) for 2 minutes prior to imaging using the Genesys imaging software. Quantification of protein levels was performed using ImageJ.

Metabolomics Analysis

Assessment of the intracellular metabolome was performed by untargeted polar and targeted nonpolar ultrahigh performance liquid chromatography coupled to mass spectrometry (UHPLC-MS) as described in (Stanford & Collins et al., 2021) by our collaborators in the Tiziani Laboratory at The University of Texas Austin.

Co-Crystal Structure of 5d & LMPTP

Co-crystallization of LMPTP in complex with Compound 5d was performed as described in (Stanford & Diaz et al., 2021) by our collaborators at the Pinkerton Laboratory at the Sanford Burnham Prebys Medical Discovery Institute.

Inhibitor IC_{50} on mutagenized LMPTP

Phosphatase assays were performed in a buffer containing 50 mM Bis-Tris pH 6.0, 1 mM dithiothreitol (DTT), and 0.01% Triton-X-100, and 5 mM para-nitrophenylphosphate (pNPP) as a substrate at room temperature. Reactions were stopped by addition of twice the reaction volume of 1M NaOH. Absorbance was measured at 405 nm, and percent activity was normalized to the activity of wells containing DMSO. IC_{50} curves were generated by fitting plots of inhibitor

concentration versus percentage of enzyme activity to a model of one-phase decay in GraphPad Prism 7.0.

Insulin-stimulated AKT Phosphorylation

Human HepG2 cells were cultured in Eagle's Minimum Essential Medium (EMEM) containing 10 % FBS, 100 U/mL penicillin and 100 µg/mL streptomycin. Cells were treated with 0.1% DMSO or 500 nM Compound 6g in 0.1% FBS-containing EMEM overnight. Following overnight 0.1% FBS/EMEM starvation, cells were stimulated with 10 nM bovine insulin for 5 minutes at 37°C in the presence of 0.1% DMSO or 500 nM Compound 6g. AKT phosphorylation was assessed by Western blotting as described above.

RESULTS

LMPTP knockout reduces subcutaneous adipocyte size *in vivo*

To examine the role of LMPTP in adipocyte biology, we generated adipocyte-specific LMPTP knockout mice using an *Acp1*-floxed *Adipoq*-Cre knockout system. We placed Cre^+ (KO) and Cre^- (WT) mice on HFD chow for 12 months, and subcutaneous (SubQ) fat pads were isolated from WT and KO mice. Our results showed that KO mice had lighter SubQ fat pads than their WT littermate counterparts (Figure 1a). Similarly, H&E staining of sections of SubQ fat pads demonstrated that a loss of LMPTP resulted in smaller adipocyte size (Figure 1b-c). Combined, these results suggest that LMPTP promotes SubQ adipocyte size in obese mice.

LMPTP promotes adipogenesis *in vitro*

To better understand the role of LMPTP in adipocytes, we sought to determine if LMPTP promotes the differentiation of preadipocytes into mature adipocytes. We isolated preadipocyte fibroblast cells from the SubQ fat pads of littermate global LMPTP KO and WT mice and subjected them to an *in vitro* differentiation assay (Scheme 1). At the end of the 10-day differentiation course, intracellular lipid levels were assessed by staining with AdipoRed. Cells from LMPTP KO mice displayed significantly reduced levels of adipogenesis as assessed by intracellular lipid accumulation (Figure 2a). Next, we assessed whether LMPTP is required for the differentiation of 3T3-L1 preadipocytes. Using cell-permeable ASOs, we knocked down LMPTP expression in 3T3-L1 undergoing the differentiation assay and found that a loss of LMPTP significantly reduced adipogenesis (Figure 2b). Similarly, we utilized a selective LMPTP inhibitor (Stanford et al., 2017), Compound 23, and found that inhibition of LMPTP

significantly reduced *in vitro* adipogenesis (Figure 2c). Taken together, these results suggest that the activity of LMPTP promotes the differentiation of preadipocytes.

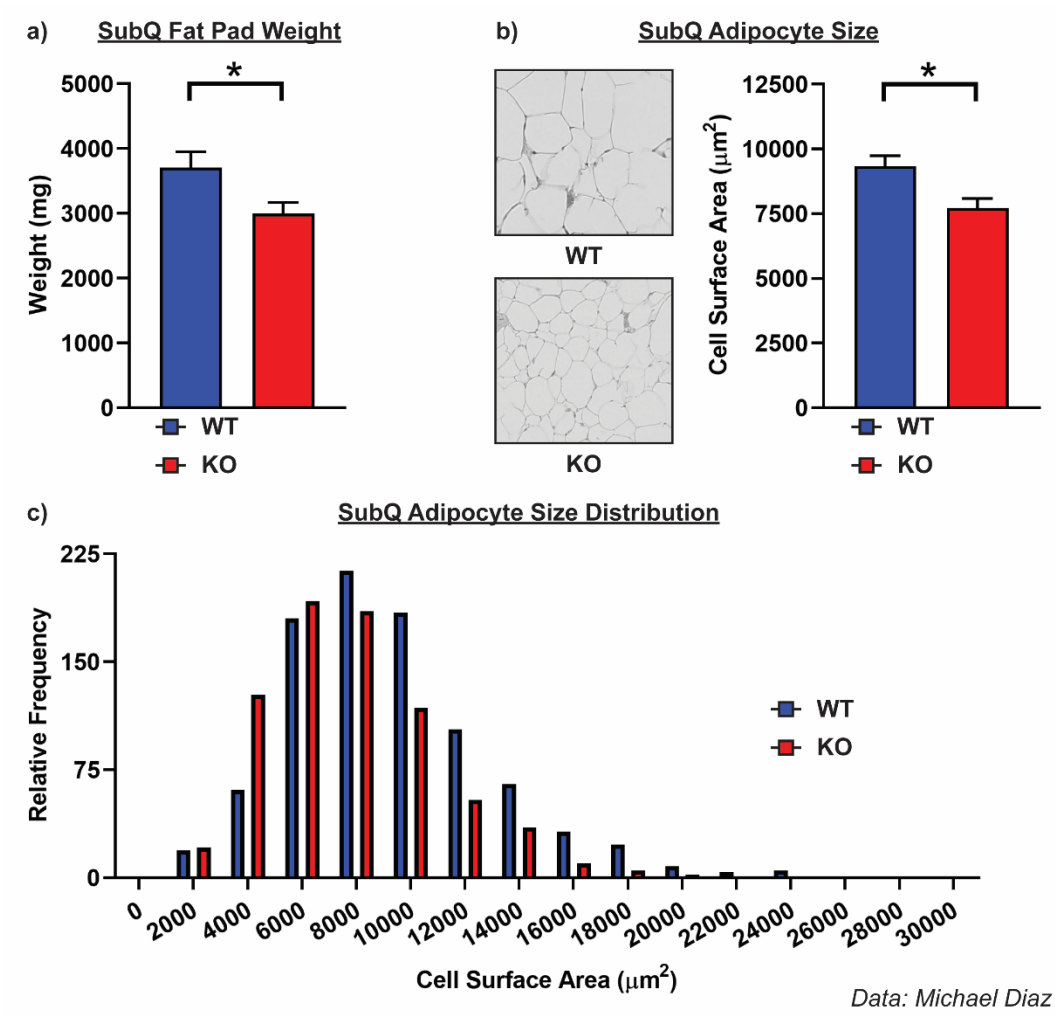

Figure 1: LMPTP knockout reduces subcutaneous adipocyte size *in vivo*. Male littermate *Acp1*-floxed adiponectin-Cre+ (KO, n=5) and Cre- (WT, n=6) mice were fed high fat diet for 12 months. (a) Mean ± SEM subcutaneous (SubQ) fat pad weight. (b-c) SubQ adipose tissue was harvested and stained with H&E and adipocyte surface area was calculated using ImageJ. (b) Mean ± SEM adipocyte surface area. (c) Frequency distribution of SubQ adipocyte sizes. (a, b) *$p < 0.05$, unpaired t-test with Welch's correction. WT, wildtype; KO, knockout. *This figure is coauthored by Zachary Holmes and Michael Diaz. Zachary Holmes is the secondary author for this figure.*

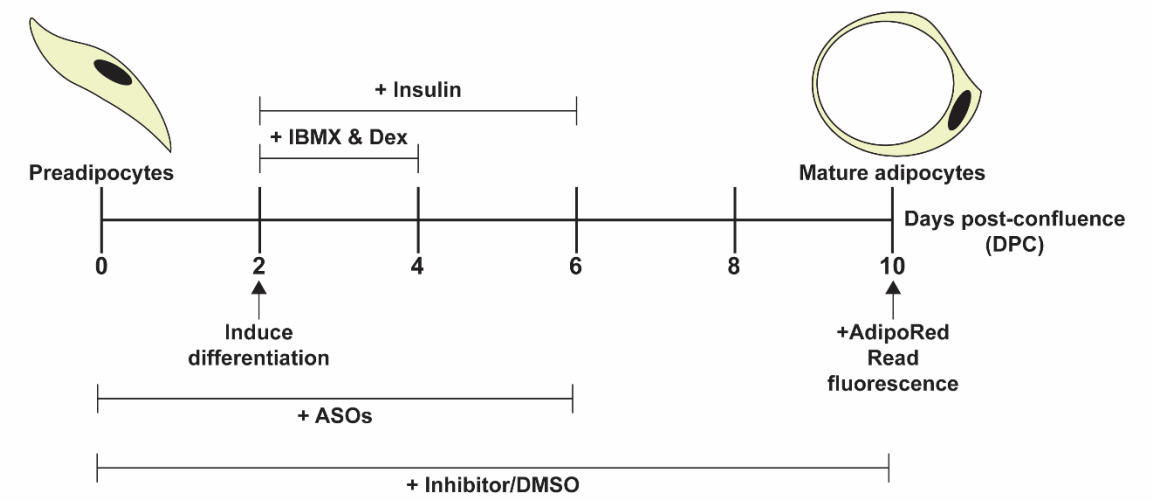

Scheme 1: Adipogenesis experimental timecourse. Preadipocyte cells were seeded in 6-well plates and grown to confluence. Starting on the day of confluence (Day 0), cells were treated with either 10 μM control ASO vs 10 μM LMPTP-targeting ASO, 10 μM Compound 23 vs DMSO, or left untreated. Every two days, the growth media was replaced and re-supplemented with the indicated additives. Two days post confluence (DPC), cells were induced to differentiate by addition of Insulin, IBMX, and Dex. On day 4 post confluence, IBMX & Dex and were removed from the growth media. On day 6, Insulin (& ASOs when applicable) was removed from the media. Cells were left to grow and differentiate until 10 DPC. Cells were then stained with AdipoRed intracellular lipid stain and cellular differentiation was quantified by measuring fluorescence.

LMPTP promotes pro-adipogenic gene expression in 3T3-L1

We hypothesized that the reduced levels of adipogenesis observed in cells lacking LMPTP activity could be due to a reduction of pro-adipogenic transcription factor expression. During the adipogenesis timecourse, expression of pro-adipogenic transcription factors is induced. The CEBP family of transcription factors act as regulators of PPARγ expression in adipocytes (Madsen et al., 2014). A diagram explaining the transcriptional regulation of pro-adipogenic genes can be found in Scheme 2. To test our hypothesis, we subjected 3T3-L1 in the presence and absence of Compound 23 to the *in vitro* adipogenesis assay and tested for the expression of pro-adipogenic transcription factors and key adipocyte genes over the 10-day differentiation process. Interestingly, we observed no effect on the expression of the gene

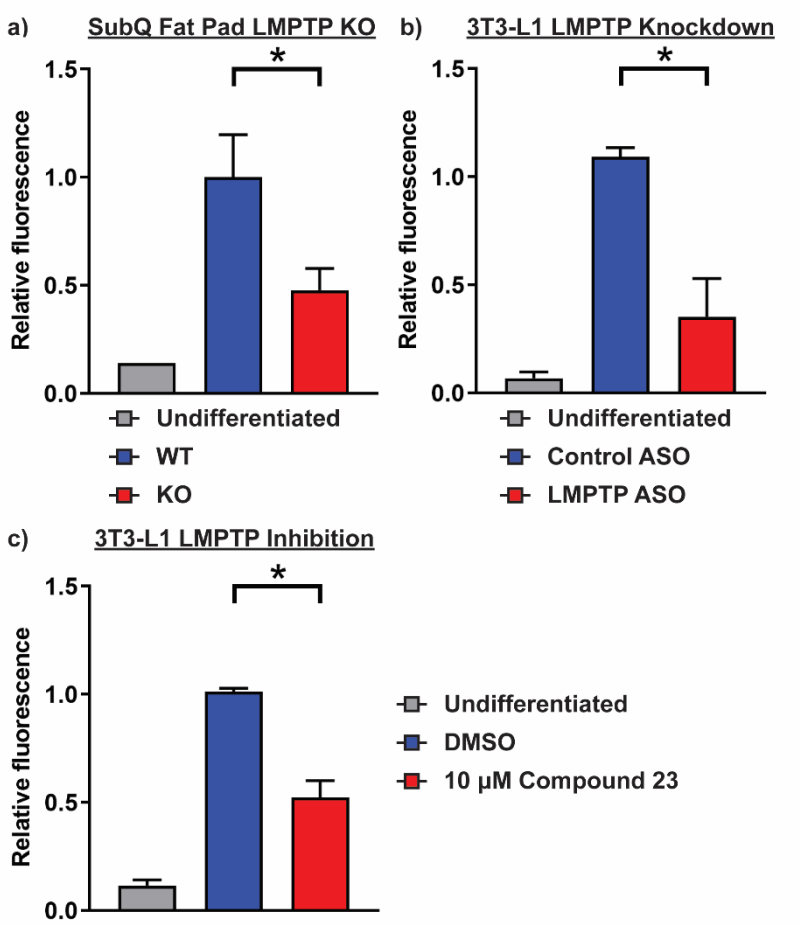

Data: Zachary Holmes, Michael Diaz, Matthew Bliss, Vida Zhang

Figure 2: LMPTP promotes adipogenesis *in vitro*. (a) Primary preadipocytes isolated from SubQ fat pads of WT (n=3) & LMPTP KO (n=4) mice were subjected to an *in vitro* adipogenesis assay. Cells from 1 WT mouse were used as an undifferentiated control. Mean ± SEM fluorescence is shown. (b-c) 3T3-L1 preadipocytes were subjected to an *in vitro* adipogenesis assay in the presence of 10 µM control non-targeting antisense oligonucleotides (ASOs) or 10 µM LMPTP-targeting ASOs (n=3) (a), or 10 µM LMPTP inhibitor Compound 23 or DMSO (n=14) (b). Mean ± SEM fluorescence is shown. (a-c) Cells were stained with AdipoRed and fluorescence was measured. Fluorescence relative to the control sample is shown; *$p < 0.05$, unpaired t-test with Welch's correction. *This figure is coauthored by Zachary Holmes, Michael Diaz, Matthew Bliss and Vida Zhang. All authors contributed equally to this figure.*

encoding the early transcription factor CEBP/β (Lee et al., 2019), yet reduced expression of the genes encoding PPARγ and CEBP/α (Figure 3). We also observed that in LMPTP-inhibited cells, there was a significant reduction in the expression of the PPARγ-dependent genes *Adipoq* and *Fas* (Figure 3). Taken together, these results demonstrate that LMPTP promotes adipogenesis at a transcriptional level, possibly through a PPARγ-dependent mechanism.

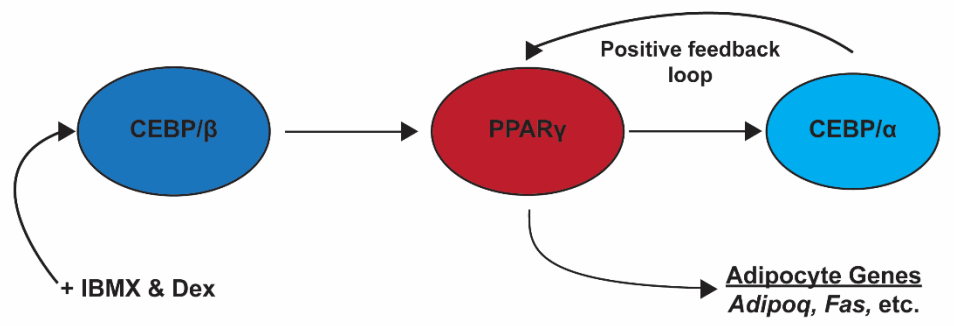

Scheme 2: Gene expression during adipogenesis. Initial expression of pro-adipogenic transcription factors is induced by IBMX & Dex in the differentiation induction cocktail. IBMX & Dex induce expression of CCAAT-enhancer binding protein isoform β (CEBP/β). The transcription factor CEBP/β promotes expression of peroxisome proliferator activated receptor gamma (PPARγ), the master regulator of genes that characterize the adipocyte phenotype. PPARγ also promotes expression of CEBP isoform α (CEBP/α), which in-turn binds to the promoter of PPARγ to further the expression of both transcription factors.

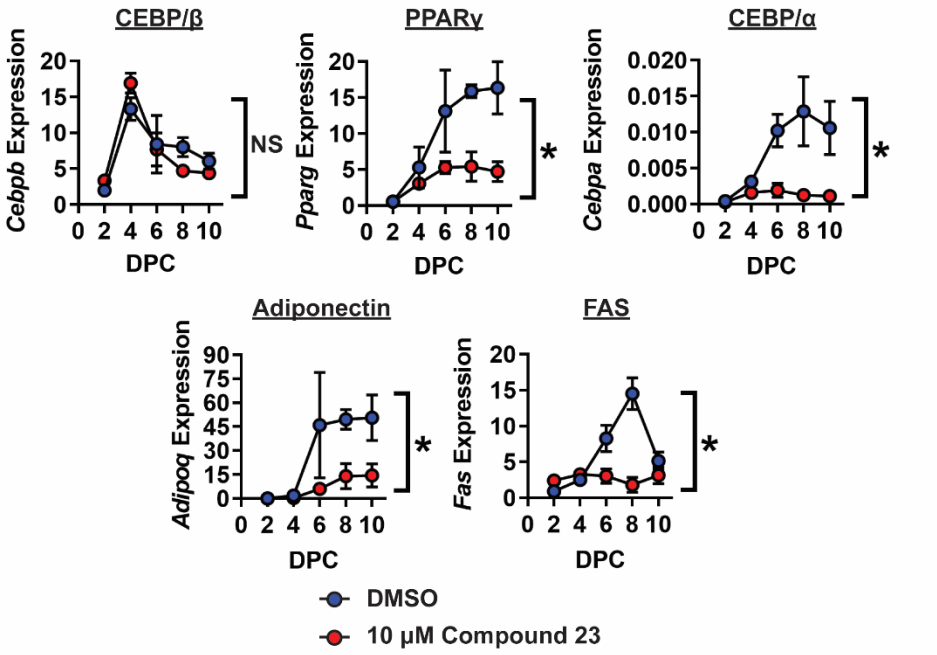

Data: Michael Diaz

Figure 3: LMPTP promotes pro-adipogenic gene expression in 3T3-L1. 3T3-L1 were subjected to an *in vitro* adipogenesis assay in the presence of 10 μM Compound 23 or DMSO. mRNA from the genes encoding the indicated proteins was measured at the indicated times by qPCR in 3 independent experiments. Mean ± SEM relative expression of the genes normalized to the housekeeping gene *Polr2a* is shown. *$p < 0.05$; NS, nonsignificant: two-way ANOVA treatment effect. DPC, days post-confluence. *This figure is coauthored by Zachary Holmes and Michael Diaz. Zachary Holmes is the secondary author for this figure.*

LMPTP inhibits basal PDGFRα signaling in 3T3-L1

LMPTP has been proposed to bind the activation loop of the PDGFR *in vitro* (Chiarugi et al., 2002), and since PDGFR signaling has also been reported to inhibit the adipogenesis of 3T3-L1 (Artemenko et al., 2005), we sought to explore a potential mechanism for LMPTP regulating adipogenesis through the PDGFR. We assessed phosphorylation of PDGFRα on activation loop residue Tyr849 in unstimulated conditions and found that LMPTP inhibition significantly increased activation of PDGFRα (Figure 4a). Next, we assessed signaling downstream of PDGFRα, and found significantly enhanced phosphorylation on activating residues of the mitogen-activated protein kinases (MAPKs) p38 and c-Jun-N-terminal kinase (JNK; Figure 4b) in response to LMPTP inhibition. Taken together, these results suggest that LMPTP inhibits PDGFRα signaling in preadipocytes.

LMPTP reduces inhibitory PPARγ Ser82 phosphorylation

In addition to regulation at the transcriptional level, PPARγ activity can be regulated by serine phosphorylation. Phosphorylation of Ser82 can inhibit the transcriptional activity of PPARγ (Yin et al., 2006). Interestingly, p38 and JNK have both been reported to phosphorylate PPARγ on Ser82 (Aouadi et al., 2006; Yin et al., 2006; Camp et al., 1999), so we assessed the phosphorylation of PPARγ in the presence and absence of Compound 23. Concomitant with the enhanced activation of p38 and JNK, we found that Compound 23-treated 3T3-L1 exhibited significantly higher levels of PPARγ Ser82 phosphorylation (pSer82) in both unstimulated cells and in cells at day 3 of the adipogenesis assay (Figure 5a-b). These results are consistent with the previously described data that suggests LMPTP regulates adipogenesis through a PPARγ-dependent pathway. Taken together, these data suggest that LMPTP is a promoter of PPARγ activity and adipogenesis, possibly through the PDGFRα signaling pathway.

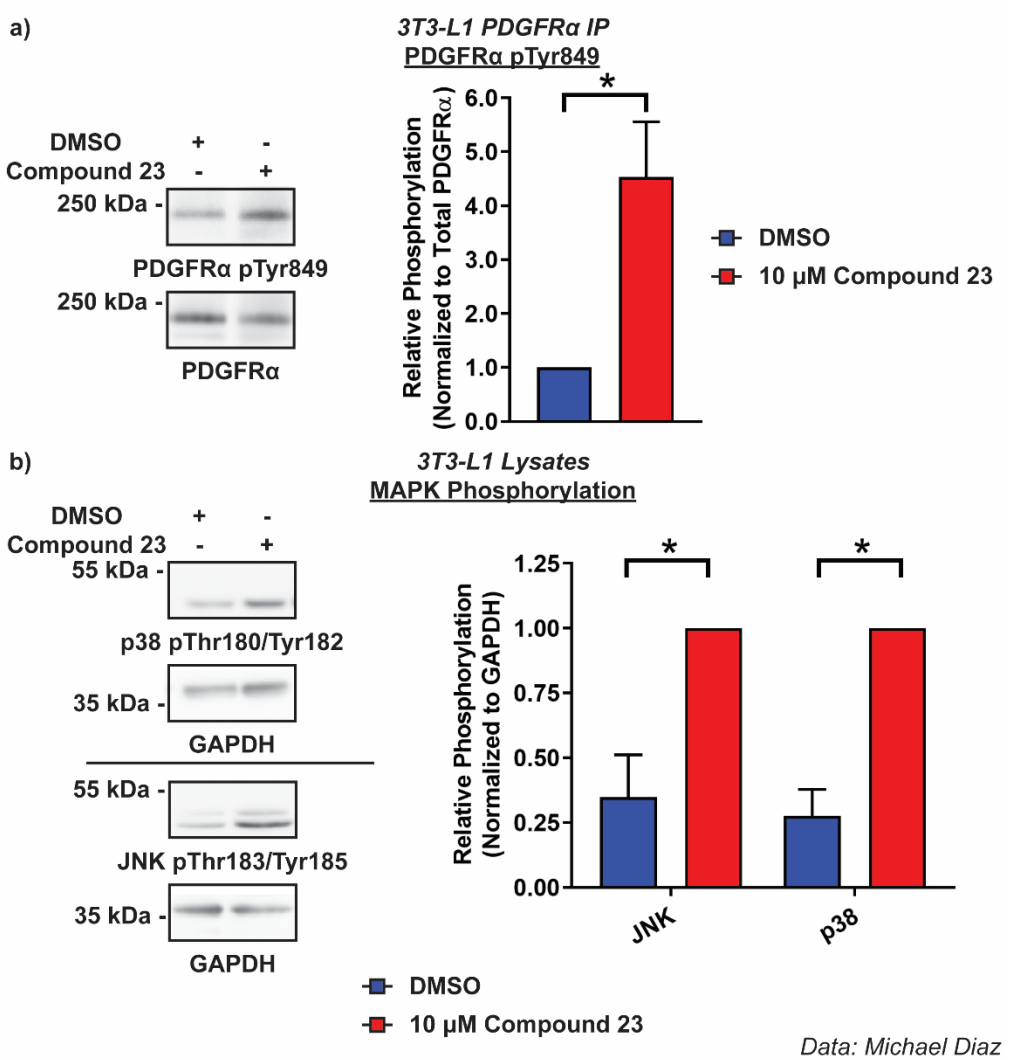

Figure 4: LMPTP inhibits basal PDGFRα signaling in 3T3-L1. 3T3-L1 were serum starved overnight in the presence of 10 μM Compound 23 or DMSO and phosphorylation of components of the PDGFRα signaling pathway were assessed by Western blotting. (a) PDGFRα was immunoprecipitated (IP) and Tyr849 phosphorylation (pTyr849) was assessed in 5 independent experiments. (b) JNK and p38 activation motif phosphorylation in cell lysates was assessed in 4 independent experiments. (a-b) Mean ± SEM phosphorylation blot signal following normalization to the indicated proteins is shown. * $p < 0.05$: unpaired t-test with Welch's correction. IP, immunoprecipitation; MAPK, mitogen activated protein kinase. *This figure is coauthored by Zachary Holmes and Michael Diaz. Zachary Holmes is the secondary author for this figure.*

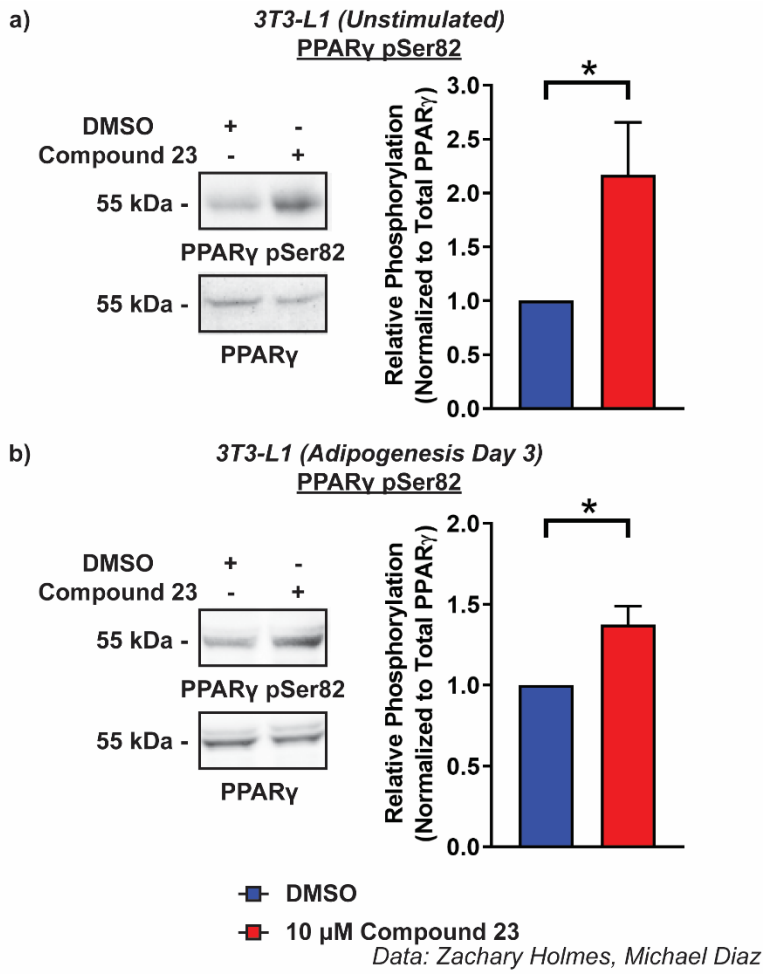

Figure 5: LMPTP reduces inhibitory PPARγ Ser82 phosphorylation. (a-b) 3T3-L1 were either serum starved and left unstimulated (a) or were subjected to an incomplete *in vitro* adipogenesis assay (b) and phosphorylation of PPARγ on Ser82 (pSer82) was assessed by Western blotting. Mean ± SEM pSer82 blot signal following normalization to total PPARγ in unstimulated 3T3-L1 (n=5) and 3T3-L1 at day 3 of adipogenesis (n=3) is shown. * $p < 0.05$: unpaired t-test with Welch's correction. *This figure is coauthored by Zachary Holmes and Michael Diaz. Zachary Holmes is the primary author for this figure.*

LMPTP inhibition alters the metabolome of differentiating 3T3-L1

To better understand the role of LMPTP in adipogenesis, we performed a metabolomic analysis of 3T3-L1 at days 2, 6, and 10 of the *in vitro* adipogenesis assay. Using UHPLC-MS based analysis, we assessed the intracellular metabolome of differentiating adipocytes in the presence or absence of Compound 23. PCA analysis revealed a stark difference between DMSO and Compound 23-treated cells at day 2 of adipogenesis, which became more extreme

throughout the 10-day differentiation process (Figure 6a). We discovered that glucose levels were significantly increased in Compound 23-treated cells, and yet there was a significant reduction in levels of glycolytic intermediates fructose-1,6-bisphosphate (Fructose 1,6BP) and phosphoenolpyruvate (PEP), as well as the glycolysis product, lactate. Additionally, we observed significantly decreased levels of 6-phosphogluconate and the reduced form of nicotinamide adenine dinucleotide phosphate (NADPH), products of the pentose phosphate pathway (PPP; Figure 6b-c). These results seem to suggest that LMPTP inhibition results in a decrease in glucose utilization.

Since glucose-6-phosphate is the first product of glycolysis and the initial substrate for the PPP, we hypothesized that increased glucose levels coupled with reduced levels of glycolysis and PPP intermediates may be due to inhibition of the first step of glycolysis. Hexokinase 2 (HK2) is the enzyme which catalyzes the phosphorylation of glucose to glucose-6-P. Interestingly, HK2 has been shown to be transcriptionally regulated by PPARγ (Panasyuk et al., 2012). We then sought to assess the expression of HK2 during the adipogenesis time course. In accordance with the reduced levels of the other PPARγ-dependent genes, we found that LMPTP inhibition significantly reduced expression of HKII, which was evident by day 6 of adipogenesis (Figure 6d). Taken together, these results suggest that treatment with an LMPTP inhibitor during preadipocyte differentiation reduces glucose metabolism.

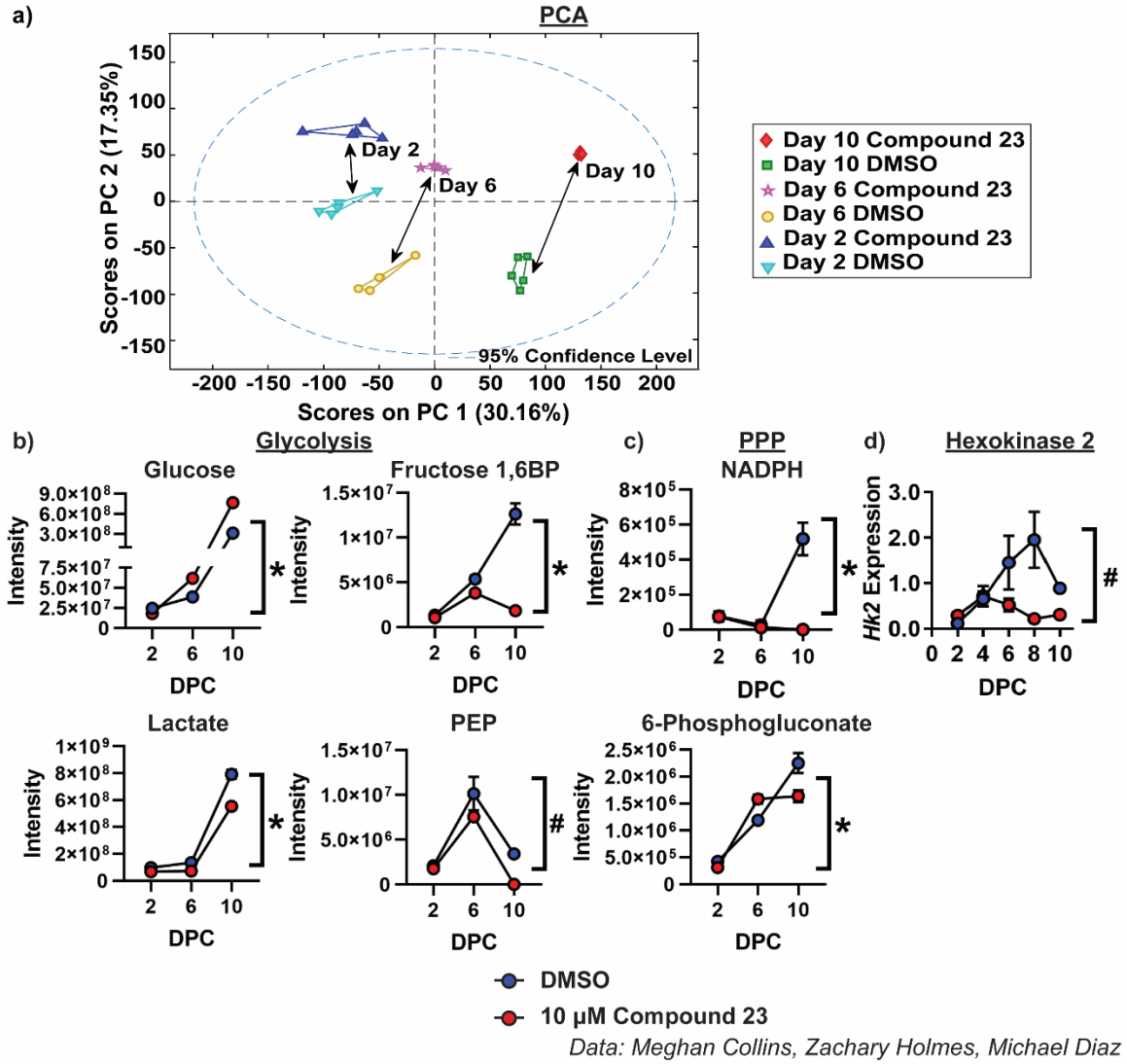

Figure 6: LMPTP inhibition alters the metabolome of differentiating 3T3-L1. (a) PCA (PC1 vs PC2) obtained from the metabolomic and fatty acid analyses of 3T3-L1 treated with 10 µM Compound 23 or DMSO at days 2, 6, and 10 of the *in vitro* adipogenesis assay. (b-c) The cellular metabolome was assessed by UHPLC-MS in differentiating the cells from (a). (b-c) Intensity of glucose, glycolytic intermediates, lactate (b), and products of the pentose phosphate pathway (PPP) (c). Mean ± SEM metabolite intensity from 5 experimental replicates is shown. (d) 3T3-L1 were subjected to an *in vitro* adipogenesis assay in the presence of 10 µM Compound 23 or DMSO. mRNA from the gene encoding hexokinase 2 (*Hk2*) was measured at the indicated times by qPCR in 3 independent experiments. Mean ± SEM relative expression of *Hk2* normalized to the housekeeping gene *Polr2a* is shown. (b-d) * $p < 0.05$: two-way ANOVA interaction effect, # $p < 0.05$: two-way ANOVA treatment effect. DPC, days post-confluence; PEP, phosphoenolpyruvate. *This figure is coauthored by Zachary Holmes, Meghan Collins, and Michael Diaz. Zachary Holmes and Meghan Collins are the primary authors for this figure and contributed equally*.

LMPTP inhibition enhances mitochondrial respiration & nucleotide synthesis in differentiating 3T3-L1

Next, we reasoned that if differentiating LMPTP inhibitor-treated 3T3-L1 experienced reduced levels of glucose metabolism, they may undergo increased mitochondrial respiration as an alternative energy source. In our metabolomic analysis, we found that Compound 23-treated cells displayed significantly reduced ratios of reduced:oxidized forms of nicotinamide adenine dinucleotide (NADH:NAD+) and Coenzyme Q_9 ($CoQ9H_2$:CoQ_9), which are redox factors whose reduced forms are substrates of the mitochondrial electron transport chain (mETC; Figure 7a). Increased levels of the oxidized forms of these mETC redox factors may be reflective of enhanced utilization of their reduced forms, suggesting increased mitochondrial respiration. Interestingly, 3T3-L1 have been demonstrated to exhibit enhanced levels of respiration during proliferation (Yao et al., 2019), and cells upregulate nucleotide synthesis during proliferation to accommodate the increased levels of DNA replication and RNA transcription (Lane & Fan, 2015). Because of this relationship, we examined nucleotide levels and found significantly increased levels of all detected nucleotides in Compound 23-treated cells compared to DMSO-treated counterparts by the end of the adipogenesis assay (Figure 7b). Taken together, our data suggest that inhibition of LMPTP alters the metabolome of differentiating 3T3-L1 to a phenotype that is more reflective of a proliferative state than a differentiating state.

Discovery of new LMPTP inhibitors

In addition to our examination of the biological role of LMPTP in adipogenesis, we have sought to develop better, more potent orally bioavailable inhibitors of LMPTP. Our lab's first series of LMPTP inhibitors have been previously described (Stanford et al., 2017), and since then we have worked on developing new inhibitors based on a new structural scaffold. Our

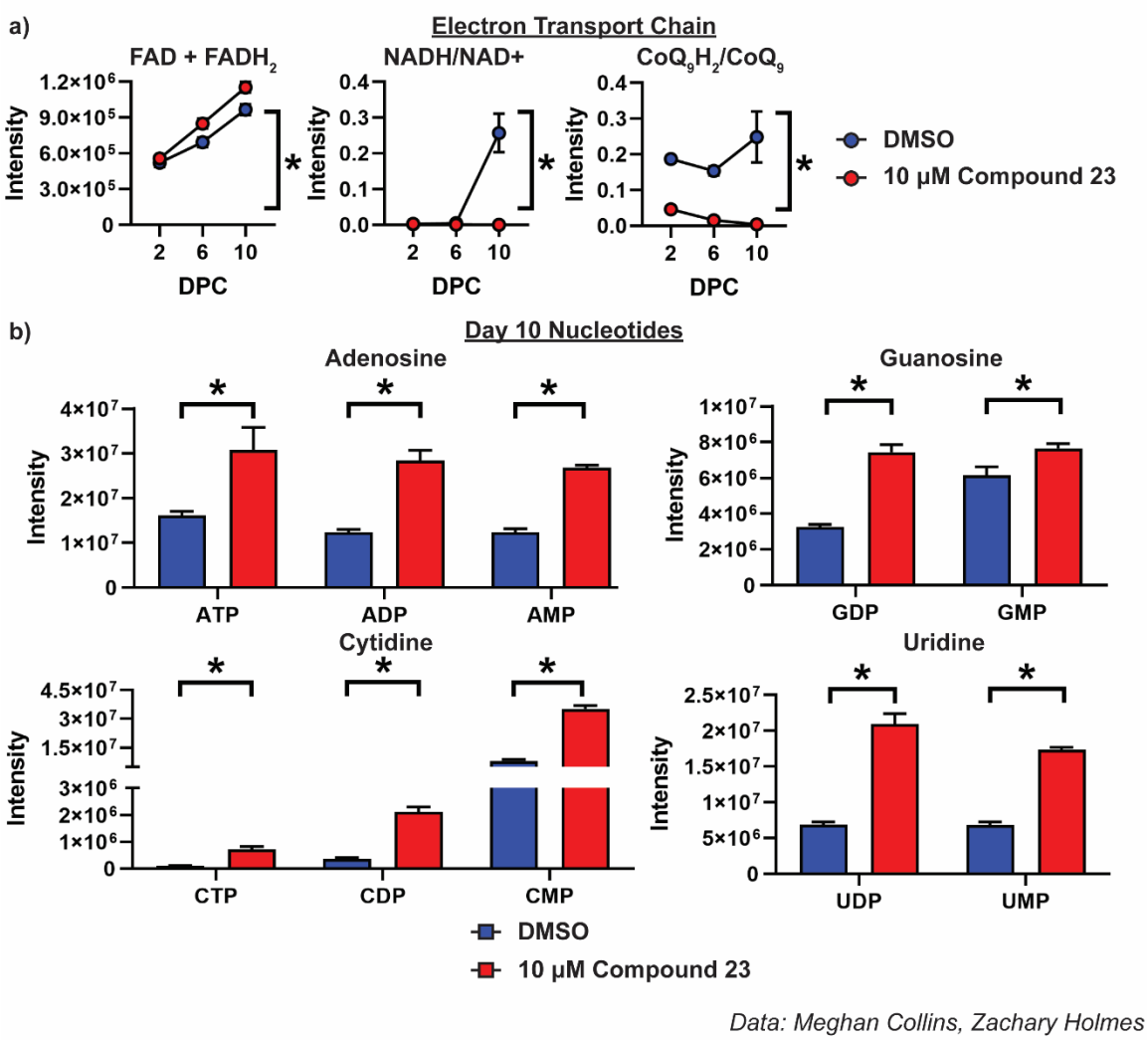

Data: Meghan Collins, Zachary Holmes

Figure 7: LMPTP inhibition enhances mitochondrial respiration & nucleotide synthesis in differentiating 3T3-L1. The cellular metabolome was assessed by UHPLC-MS in differentiating 3T3-L1 in the presence of 10 µM Compound 23 or DMSO. (a) Intensity of the total $FAD+FADH_2$ pool & redox ratios of NADH & CoQ_9H_2. (b) Intensity of all nucleotides detected by UHPLC-MS at day 10 of adipogenesis. (a-b) Mean ± SEM intensity from 5 experimental replicates is shown. (a) * $p < 0.05$: two-way ANOVA treatment effect. (b) * $p < 0.05$: unpaired t-test with Welch's correction. DPC, days post-confluence. *This figure is coauthored by Zachary Holmes and Meghan Collins and both authors contributed equally.*

chemist collaborators at Sanford Burnham Prebys Medical Discovery Institute developed a series of LMPTP inhibitors using a purine-based scaffold, a structural moiety that interestingly has been previously shown to be an activator of LMPTP (Caselli et al., 2016). A summary of the potency of the main analogs from this series of inhibitors is described in Table 2. Compared to Compound 23 in our previous series of inhibitors, these new compounds display a remarkable

Table 2: New LMPTP inhibitor IC_{50}s

Compound #	IC_{50} (μM)*
3	0.239 ± 0.053 (72)
5d	0.020 ± 0.005 (4)
6g	0.083 ± 0.006 (4)
6h	0.006 ± 0.001 (12)
* Mean ± SEM (n)	

increase in potency, with the IC_{50} of Compound 6h reaching as low as 6 nM, roughly 130-times more potent than Compound 23's reported 800 nM IC_{50} (Stanford et al., 2017). Additionally, inhibitors in this series displayed remarkable selectivity for LMPTP over other phosphatases. We tested Compound 6g at a concentration of 40 μM, more than 1000-times the reported IC_{50}, and we did not observe more than 50% inhibition of any other tested phosphatases (Stanford & Diaz et al., 2021).

Co-crystal structure of LMPTP & Compound 5d

A co-crystal structure of Compound 5d with human LMPTP A revealed that Compound 5d binds to LMPTP at the entrance of the catalytic pocket (Figure 8). The aminopurine core of this inhibitor series contributes to a significant portion of the direct interactions between the inhibitor and LMPTP, including pi-stacking with the side chain of Tyr131, a hydrophobic interaction with Leu13, and hydrogen bonding with the Asp129. Asp129 of LMPTP additionally interacts with the o-tolyl group of Compound 5d, as one end of this group is found at a van der Waals distance from both Asp129 and Tyr132. This interaction may also help to explain the

expected increase in potency when the aminopurine core of these inhibitors are substituted at the 8 position compared to comparative unsubstituted analogs. Also apparent is the interaction between the dichlorobenzyl ring of Compound 5d, which contributes to pi-stacking with Tyr49 of LMPTP in a similar fashion to the aminopurine core with Tyr131.

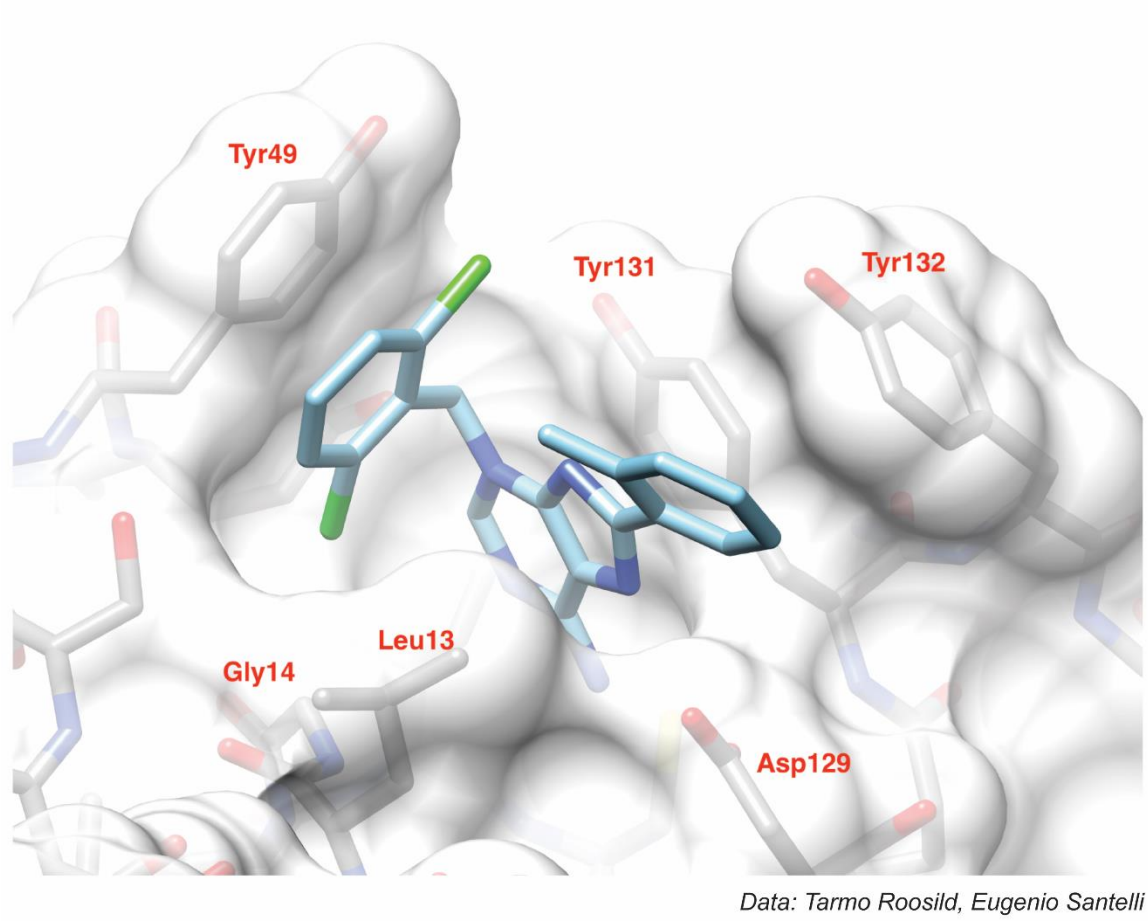

Figure 8: Co-crystal structure of LMPTP & 5d. Model of Compound 5d (light blue) in the substrate binding site of LMPTP. The protein is shown as a solvent-accessible surface in stick representation (gray). Figure was generated using Chimera. PDB: 7KH8. *This figure was used with permission from Eugenio Santelli and Anthony Pinkerton on behalf of Tarmo Roosild.*

New LMPTP inhibitors rely on Tyr131 for inhibition

In order to validate the proposed interactions set forth by our co-crystal structure, we sought to test the importance of Tyr131 and Tyr132 by performing site-directed mutagenesis and measuring the effect on the IC_{50} of Compounds 5d and 6g. The component of these tyrosine residues that contribute to interactions with the compounds is the aromatic ring on their side-chains. To effectively assess the importance of the aromatic rings in mediating compound binding and inhibition, we assessed the IC_{50}s of these inhibitors in WT LMPTP A and tyrosine to alanine (Y/A) mutants. As expected, mutation of either tyrosine residue reduced the ability of either compound to inhibit LMPTP (Figure 9). In support of the proposed co-crystal structure, disruption of the strong interaction of pi-stacking between the purine core of these inhibitors and the aromatic side chain of Tyr131 by mutagenesis blocked inhibition entirely. Y132A mutagenesis also reduced inhibitor potency but to a lesser extent, which is reflective of the inherently weaker nature of the proposed interaction with this active-site residue. In summary, our data helps to validate our co-crystal structure, as Y/A mutagenesis reduced compound-mediated inhibition in a manner that supports the proposed interactions.

6g enhances insulin-stimulated AKT phosphorylation in HepG2

One of the primary goals of this search for better inhibitors is to improve the tools with which can study LMPTP. Because of this, it is necessary that these inhibitors are useful in cell-based assays in addition to being highly potent *in vitro*. With this in mind, we sought to determine if these new inhibitors were viable in cells. Based on pharmacokinetic analysis from a panel of our inhibitors in mice, we discovered that Compound 6g had the best combination of potency and bioavailability (Stanford & Diaz et al., 2021). Because of this, we chose to proceed

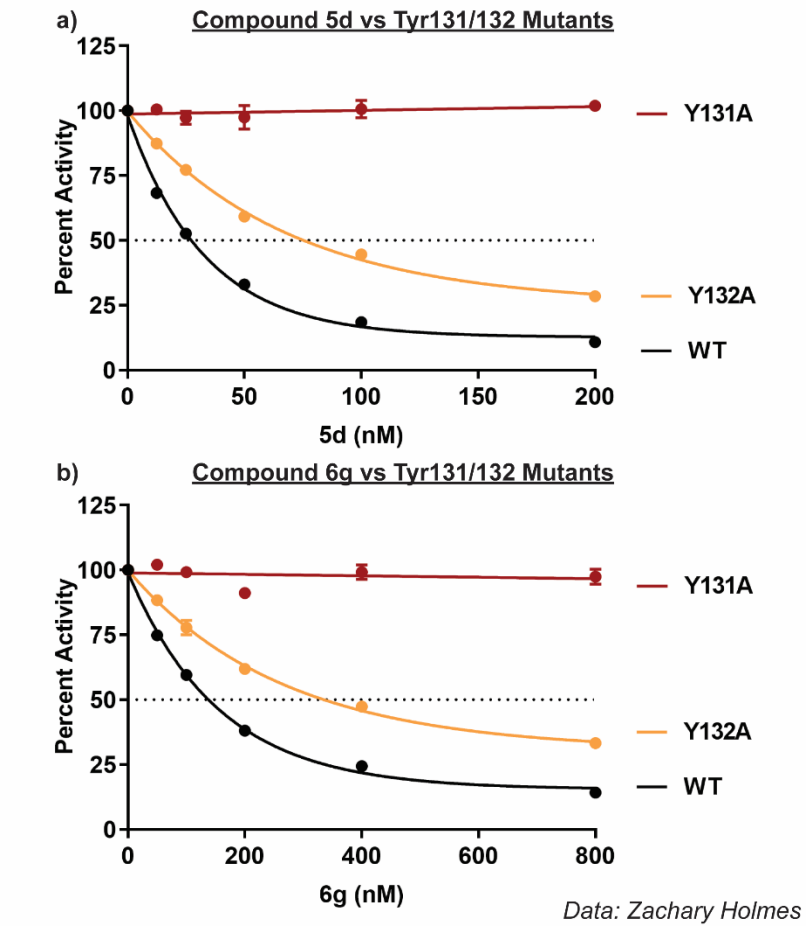

Figure 9: New LMPTP inhibitors rely on Tyr131 for inhibition. (a-b) Mutagenized LMPTP proteins with activity equal to 20 nM WT LMPTP A were used to compare hydrolysis of 5 mM para-nitrophenyl phosphate (pNPP) in the presence of increasing concentrations of Compound 5d (a) and Compound 6g (b). Mean ± SEM percent activity from 2 independent experiments is shown. For the Y131A mutant, lines shown are fit to linear regression. For WT and Y132A LMPTP, lines shown are fit to a model of one-phase decay. *Zachary Holmes is the primary author of this figure.*

with Compound 6g for testing in cells. We have previously demonstrated that LMPTP inhibition enhances liver insulin signaling (Stanford et al., 2017), so to gauge the viability of Compound 6g in cells, we assessed insulin-stimulated AKT phosphorylation in HepG2 hepatocytes. Our data showed that treatment with 500 nM 6g, a concentration that is 20-times less than the 10 μM Compound 23 treatment used in previous cell-based assays resulted in a significant increase in insulin-stimulated AKT phosphorylation. This result confirms that Compound 6g is effective in cells at a concentration much lower than our previous series of inhibitors.

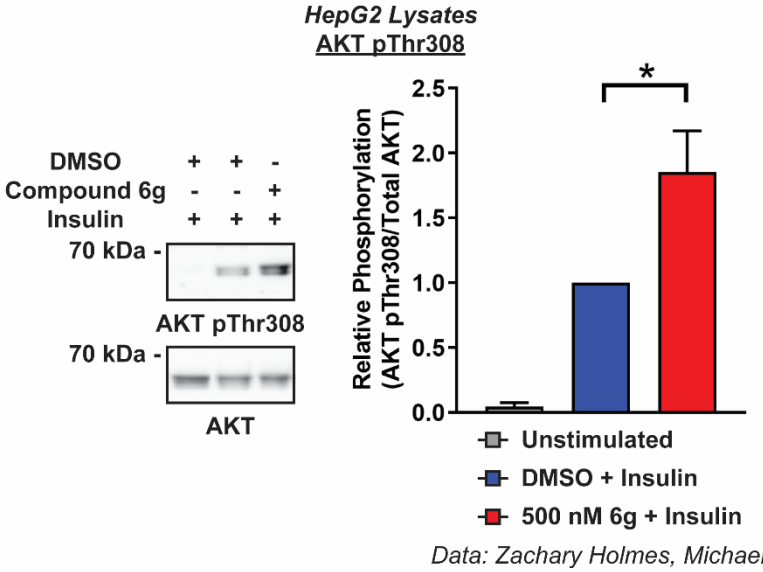

Data: Zachary Holmes, Michael Diaz

Figure 10: 6g enhances insulin-stimulated AKT phosphorylation in HepG2. HepG2 hepatocytes were serum-starved overnight in the presence of 500 nM Compound 6g or DMSO. Cells were stimulated with 10 nM bovine insulin for 5 minutes at 37°C in the presence of 500 nM Compound 6g or DMSO before lysing, and AKT Thr308 phosphorylation (pThr308) in lysates was assessed by Western blotting. Mean ± SEM pThr308 blot signal following normalization to total AKT from 8 independent replicates is shown. * $p < 0.05$: unpaired t-test with Welch's correction. *This figure is coauthored by Zachary Holmes and Michael Diaz. Zachary Holmes is the primary author for this figure.*

DISCUSSION

In this study, we investigated the role of LMPTP in adipocyte biology and advanced the search for a viable selective inhibitor of the phosphatase. Our lab has previously shown that LMPTP promotes the severity of obesity-induced diabetes in mice (Stanford et al., 2017), and this investigation provides further evidence for the role of LMPTP in obesity-related pathology. To explore the role of LMPTP in adipocyte biology, we generated *Adipoq*-Cre LMPTP knockout mice to selectively delete LMPTP in adipocytes. Our results demonstrated that a lack of LMPTP in adipose tissue reduces SubQ adipocyte size. To determine if LMPTP plays a role in the differentiation of adipocytes, we subjected multiple preadipocyte cell lines lacking LMPTP activity or expression to an *in vitro* adipogenesis assay. Consistent with the observed effect in our *Adipoq*-Cre mice, preadipocytes lacking LMPTP activity or expression displayed a significant reduction in *in vitro* differentiation. We further demonstrated that the lack of differentiation is reflected in a reduction in gene expression of the pro-adipogenic transcription factor PPARγ, as well as many pro-adipogenic PPARγ-dependent genes. In an effort to understand how LMPTP promotes adipogenesis, we demonstrated that LMPTP is a negative regulator of basal PDGFRα signaling, as inhibition of LMPTP enhanced unstimulated PDGFRα phosphorylation on an activating Tyr residue, as well as promoted activation of the downstream p38 and JNK MAPKs. In accordance with previous studies, we showed that enhanced activation of p38 and JNK is accompanied by enhanced phosphorylation of PPARγ on the inhibitory Ser82 residue. We therefore proposed a model wherein LMPTP promotes adipogenesis by dephosphorylating the PDGFRα, thereby blocking the activation of p38 and JNK and relieving suppression of PPARγ by Ser82 phosphorylation (Scheme 3). We believe that relieving PPARγ inhibition poises it to induce the transcriptional program required for adipogenesis in response

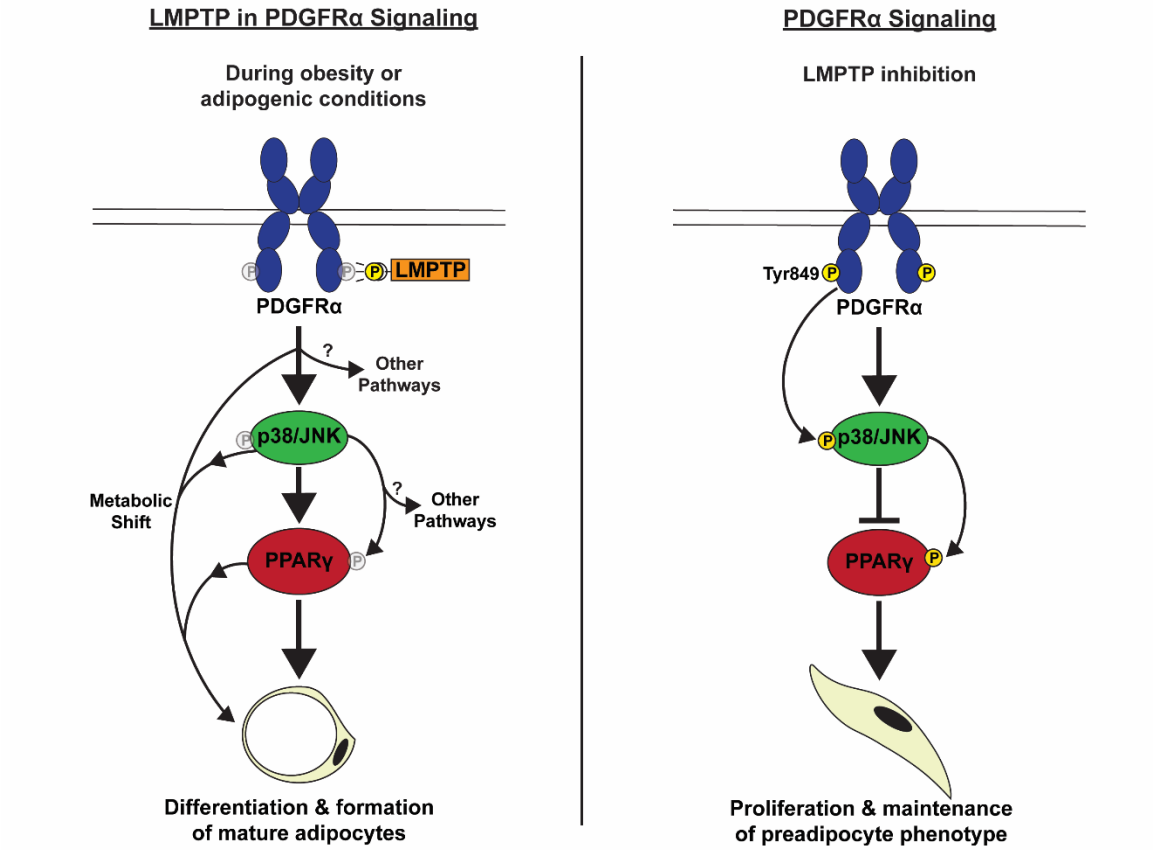

Scheme 3: The proposed role of LMPTP in adipogenesis. PDGF signaling promotes activation of the p38 and JNK MAPK proteins which phosphorylate PPARγ on an inhibitory residue. Therefore active PDGF signaling may inhibit adipogenesis by blocking the transcription of pro-adipogenic genes. Our model predicts that LMPTP dephosphorylates the PDGFRα, resulting in a reduction in inhibitory PPARγ phosphorylation, allowing for the expression of mature adipocyte genes.

to obesity or adipogenic stimulation. We do not however exclude the possibility of further mechanisms downstream of PDGFRα signaling that may contribute to the observed effect on adipogenesis. To conclude our characterization of the role of LMPTP in adipogenesis, we assessed the metabolome of differentiating 3T3-L1 throughout the 10-day adipogenesis time course. We discovered that preadipocytes treated with Compound 23 exhibited a reduction in glucose utilization as evidenced by a significant decrease in glycolytic intermediates, lactate, and of products of the pentose phosphate pathway (PPP). Additionally, we provided evidence to

suggest that LMPTP-inhibited cells exhibit a phenotype that more closely approximates that of a proliferative state than a differentiating state.

Finally, we helped to characterize a new screening of potential LMPTP inhibitors from our collaborators at Sanford Burnham Prebys Medical Discovery Institute. This new series of inhibitors has a purine-based backbone, which is a novel structure when compared to our previously used series of inhibitors which includes Compound 23. These inhibitors displayed substantially enhanced potency against LMPTP while also maintaining a staggering selectivity when compared to other tested phosphatases (Stanford & Diaz et al., 2021). We demonstrated through co-crystallization and analysis on mutagenized LMPTP that Tyr131 and Tyr132 contribute to interactions with this series of inhibitors. Lastly, we demonstrated that Compound 6g from this series is viable in cell-based assays at a remarkably reduced concentration compared to Compound 23 from the previous series of LMPTP inhibitors.

With respect to our findings for the role of LMPTP in adipogenesis, we believe that several key pieces of evidence support our theory that LMPTP promotes adipogenesis through a PDGFRα-dependent mechanism. Our finding that LMPTP inhibition enhances PDGFRα phosphorylation on an activating tyrosine residue in unstimulated cells provides evidence for the possibility that LMPTP acts directly on the receptor. LMPTP has previously been reported to regulate PDGFR tyrosine phosphorylation in fibroblasts (Chiarugi et al., 2002; Cirri et al., 1998). Additionally, previous researchers have demonstrated that mouse fibroblasts overexpressing LMPTP exhibit reduced PDGFR tyrosine phosphorylation (Chiarugi et al., 2001), providing further evidence that LMPTP may act on the PDGFR directly. More broadly, LMPTP has previously been reported by our lab to regulate insulin receptor signaling (Stanford et al., 2017). Both the insulin receptor and the PDGFR are receptor tyrosine kinases (RTK), so results from

our lab seem in-line with the previously reported role of LMPTP in regulating RTK signaling (Caselli et al., 2016).

Our theory that LMPTP regulates adipogenesis through a PDGFR-dependent pathway is also in accordance with the reported role of PDGFR signaling in WAT development. It has been shown that constitutively active PDGFRα signaling inhibits WAT formation in mice (Sun et al., 2017). Additionally, a microarray analysis of mature WAT from fat-specific insulin receptor KO mice showed that larger adipocytes had reduced PDGFR expression compared to smaller adipocytes (Bluher et al., 2004). Taken together, these findings provide evidence for our model in which PDGFR signaling is antiadipogenic. It has also been reported that PDGFRs are downregulated early after addition of adipogenesis-inducing stimuli (Vaziri & Faller, 1996), which suggests that in adipocytes, the loss of PDGFRs serves to reduce the antiadipogenic effect of PDGFR signaling. It therefore follows that LMPTP inhibition which enhances PDGFRα signaling should also reduce adipogenesis, which we observe here.

Our proposed model in which LMPTP regulates adipogenesis through a PPARγ dependent mechanism is also strongly supported by our data. As seen in Scheme 2, PPARγ acts as a master regulator of adipogenesis by directly regulating expression of the pro-adipogenic transcription factor CEBP/α (Madsen et al., 2014; Ying et al., 2006) as well as key adipocyte genes encoding adiponectin (*Adipoq*) and fatty acid synthase (*Fas*) (Ferré, 2004, Lee et al., 2018). We observed that while early induction of PPARγ around day 4 was only minimally affected, expression of PPARγ in the latter stages of adipogenesis was strongly inhibited (Figure 3). Expression of CEBP/β can be induced by addition of cAMP or glucocorticoids (Merrett et al., 2020), which is achieved by IBMX and Dex respectively, both of which are utilized in the early adipogenic stimulation cocktail. In our results, we found that expression of CEBP/β is unaffected

by LMPTP inhibition, which helps explains the initial jump in PPARγ expression, as it has been previously shown that ectopic expression of CEBP/β in NIH-3T3 cells is sufficient to induce PPARγ expression (Wu et al., 1995). Also contributing to the expression of PPARγ is insulin (Rieusset et al., 1999), which is clearly evidenced by the fact that expression of PPARγ in Compound 23-treated cells plateaus after insulin is removed from the growth media at day 6 (Figure 3). Since early PPARγ expression that typically follows CEBP/β induction and insulin stimulation is unaffected, we reasoned that reduced expression of PPARγ and PPARγ-dependent genes might therefore be explained by a lack of its transcriptional activity, which is supported by our data depicting enhanced pSer82 of PPARγ in Compound 23-treated cells. If PPARγ is inactive, it cannot promote expression of CEBP/α, which would in-turn reduce its own expression (Ying et al., 2006) and expression of all PPARγ-dependent genes. Given that the phenotype of enhanced inhibitory phosphorylation of PPARγ in Compound 23-treated cells holds true through induction of adipogenesis (Scheme 1; Figure 5b), we believe this line of reasoning to be very convincing.

In final support of our model for the role of LMPTP in adipogenesis is the line of evidence connecting LMPTP to that of a proliferative phenotype. In our examination of the metabolome of differentiating 3T3-L1, we discovered that Compound 23-treated cells exhibited significantly reduced glucose utilization, which led us to theorize that these cells were undergoing enhanced mitochondrial respiration as an alternative energy source. In accordance with this, we observed decreased ratios of the reduced:oxidized forms of NADH:NAD+ & CoQ_9H_2:CoQ_9 (Figure 7). Since the reduced forms of these electron carriers are utilized early in the electron transport, we believe the decreased ratios are evidence of enhanced utilization of this pathway. To that effect, it has been previously reported that 3T3-L1 display enhanced levels of

mitochondrial respiration during proliferation (Yao et al., 2019), which is consistent with our idea that LMPTP-inhibited cells exhibit a more proliferative phenotype than normal differentiating adipocytes. In further support of this theory, our Compound 23-treated cells also exhibit significantly enhanced levels of all nucleotides detected in the UHPLC-MS analysis, a phenotype that is well characterized alongside proliferation (Lane & Fan, 2015). Finally, it has been well-characterized that PDGF signaling promotes proliferation (Berti et al., 1994). Our data are consistent with these findings, and we therefore promise a model in which LMPTP promotes adipogenesis by dephosphorylating the PDGFRα, reducing the proliferative effect of PDGF signaling and relieving inhibitory phosphorylation of PPARγ (Scheme 3).

In our efforts to better understand the biological relevance of LMPTP in diseases, we have sought to develop better, more potent inhibitors of LMPTP. In this study, we characterized a new purine-based series of LMPTP inhibitors. We demonstrated through co-crystallization and site-directed mutagenesis that Tyr131 of LMPTP plays a critical role in compound binding to the amino-purine backbone of this new series of inhibitors. Mutation of Tyr131 and Y132 to alanine blocked the ability of these compounds to inhibit entirely, or reduced inhibitor potency by at least half respectively. Observed effects were less significant when Tyr132 is the mutated residue, which is consistent with the predicted importance of the two Tyr residues according to our co-crystal structure. Finally, we tested Compound 6g in HepG2 hepatocytes and found that inhibition of LMPTP via addition of 500 nM 6g significantly enhanced insulin-stimulated AKT phosphorylation. These results are consistent with our previous findings that LMPTP inhibition enhances liver insulin signaling (Stanford et al., 2017), and this result further highlights the importance of LMPTP as a critical regulator of insulin signaling and diabetes in obesity.

REFERENCES

Accili, D., & Taylor, S. I. (1991). Targeted inactivation of the insulin receptor gene in mouse 3T3-L1 fibroblasts via homologous recombination. *Proceedings of the National Academy of Sciences of the United States of America*, 88(11), 4708–4712. https://doi.org/10.1073/pnas.88.11.4708

Alonso, A., Nunes-Xavier, C.E., Bayón, Y., Pulido, R. (2016) The extended family of protein tyrosine phosphatases. *Methods in Molecular Biology*, 1447, 1-23. https://doi.org/10.1007/978-1-4939-3746-2_1

Aouadi, M., Laurent, K., Prot, M., Le Marchand-Brustel, Y., Binetruy, B., Bost, F. (2006). Inhibition of p38MAPK increases adipogenesis from embryonic to adult stages. *Diabetes*, 55(2), 281–289. https://doi.org/10.2337/diabetes.55.02.06.db05-0963

Artemenko, Y., Gagnon, A., Aubin, D., Sorisky, A. (2005). Anti- adipogenic effect of PDGF is reversed by PKC inhibition. *Journal of Cellular Physiology*, 204(2), 646–653. https://doi.org/10.1002/jcp.20314

Berti, A., Rigacci, S., Raugei, G., Degl'Innocenti, D., Ramponi, G. (1994). Inhibition of cellular response to platelet-derived growth factor by low M(r) phosphotyrosine protein phosphatase overexpression. *FEBS Letters*, 349(1), 7–12. https://doi.org/10.1016/0014-5793(94)00620-2

Bluher, M., Patti, M.E., Gesta, S., Kahn, B.B., Kahn, C.R. (2004). Intrinsic heterogeneity in adipose tissue of fat-specific insulin receptor knock-out mice is associated with differences in patterns of gene expression. *Journal of Biological Chemistry*, 279(30), 31891–31901. https://doi.org/10.1074/jbc.M404569200

Bottini, E., Lucarini, N., Gerlini, G., Finocchi, G., Scire, G., Gloria-Bottini, F. (1990). Enzyme polymorphism and clinical variability of diseases: Study of acid phosphatase locus 1 (ACP1) in obese subjects. *Human Biology*, 62(3), 403–411.

Bottini, N., MacMurray, J., Peters, W., Rostamkhani, M., Comings, D. E. (2002). Association of the acid phosphatase (ACP1) gene with triglyceride levels in obese women. *Molecular Genetics and Metabolism*, 77(3), 226–229. https://doi.org/10.1016/s1096-7192(02)00120-8

Camp, H.S., Tafuri, S.R., & Leff, T. (1999). c-Jun N-terminal kinase phosphorylates peroxisome proliferator-activated receptor-gamma1 and negatively regulates its transcriptional activity. *Endocrinology*, 140(1), 392–397. https://doi.org/10.1210/endo.140.1.6457

Caselli, A., Paoli, P., Santi, A., Mugnaioni, C., Toti, A., Camici, G., Cirri, P. (2016). Low molecular weight protein tyrosine phosphatase: Multifaceted functions of an evolutionarily conserved enzyme. *Biochimica et Biophysica Acta/General Subjects*, 1864(10), 1339–1355. https://doi.org/10.1016/j.bbapap.2016.07.001

Chiarugi, P. (2001). The redox regulation of LMW-PTP during cell proliferation or growth inhibition. *IUBMB Life*, 52(1-2), 55–59. https://doi.org/10.1080/15216540252774775

Chiarugi, P., Cirri, P., Marra, F., Raugei, G., Camici, G., Manao, G., Ramponi, G. (1997). LMW-PTP is a negative regulator of insulin-mediated mitotic and metabolic signaling. *Biochemical and Biophysical Research Communications*, 282(2), 676-682. https://doi.org/10.1006/bbrc.1997.7355

Chiarugi, P., Cirri, P., Taddei, M. L., Giannoni, E., Fiaschi, T., Buricchi, F., Camici, G., Raugei, G., Ramponi, G. (2002). Insight into the role of low molecular weight phosphotyrosine phosphatase (LMW-PTP) on platelet-derived growth factor receptor (PDGF-r) signaling. LMW-PTP controls PDGF-r kinase activity through Tyr-857 dephosphorylation. *Journal of Biological Chemistry*, 277(40), 37331–37338. https://doi.org/10.1074/jbc.M205203200

Chooi, Y.C., Ding, C., & Magkos, F. (2019). The epidemiology of obesity. *Metabolism: Clinical and Experimental*, 92, 6–10. https://doi.org/10.1016/j.metabol.2018.09.005

Cirri, P., Chiarugi, P., Taddei, L., Raugei, G., Camici, G., Manao, G., Ramponi, G. (1998). Low molecular weight protein-tyrosine phosphatase tyrosine phosphorylation by c-Src during platelet-derived growth factor-induced mitogenesis correlates with its subcellular targeting. *Journal of Biological Chemistry*, 273(49), 32522–32527. https://doi.org/10.1074/jbc.273.49.32522

Ferré, P. (2004). The biology of peroxisome proliferator-activated receptors. *Diabetes*, 53(1), S43-S50. https://doi.org/10.2337/diabetes.53.2007.S43

Hales C.M., Carroll M.D., Fryar C.D., Ogden C.L. (2020) Prevalence of obesity and severe obesity among adults: United States, 2017–2018. *NCHS Data Brief*, 360.

Johnson, T.O., Ermolieff, J., Jirousek, M.R. (2002). Protein tyrosine phosphatase 1b inhibitors for diabetes. *Nature Reviews Drug Discovery*, 1, 696−709. https://doi.org/10.1038/nrd895

Lane, A.N., & Fan, T.W. (2015). Regulation of mammalian nucleotide metabolism and biosynthesis. *Nucleic Acids Research*, 43(4), 2466–2485. https://doi.org/10.1093/nar/gkv047

Lee, J.E., Schmidt, H., Lai, B., Ge, K. (2019). Transcriptional and epigenomic regulation of adipogenesis. *Molecular and Cellular Biology*, 39(11), e00601-18. https://doi.org/10.1128/MCB.00601-18

Lee, Y.K., Park, J.E., Lee, M., Hardwick, J.P. (2018). Hepatic lipid homeostasis by peroxisome proliferator-activated receptor gamma 2. *Liver Research*, 2(4), 209-215. https://doi.org/10.1016/j.livres.2018.12.001

Lucarini, N., Antonacci, E., Bottini, N., Gloria-Bottini, F. (1997). Low- molecular-weight acid phosphatase (ACP1), obesity, and blood lipid levels in subjects with non-insulin-dependent diabetes mellitus. *Human Biology*, 69(4), 509–515.

Madsen, M.S., Siersbæk, R., Boergesen, M., Nielsen, R., Mandrup, S. (2014). Peroxisome proliferator-activated receptor γ and C/EBPα synergistically activate key metabolic adipocyte genes by assisted loading. *Molecular and Cellular Biology*, 34(6), 939-954. https://doi.org/10.1128/MCB.01344-13

Merrett, J.E., Bo, T., Psaltis, P.J., Proud, C.G. (2020) Identification of DNA response elements regulating expression of CCAAT/enhancer-binding protein (C/EBP) β and δ and MAP kinase-interacting kinases during early adipogenesis. *Adipocyte*, 9(1), 427-442. https://doi.org/10.1080/21623945.2020.1796361

Musi, N., Goodyear, L.J. (2006). Insulin resistance and improvements in signal transduction. *Endocrine*, 29, 73−80. https://doi.org/10.1385/ENDO:29:1:73.

Panasyuk, G., Espeillac, C., Chauvin, C., Pradelli, L.A., Horie, Y., Suzuki, A., Annicotte, J.S., Fajas, L., Foretz, M., Verdeguer, F., Pontoglio, M., Ferré, P., Scoazec, J.Y., Birnbaum, M.J., Ricci, J. E., Pende, M. (2012). PPARgamma contributes to PKM2 and HK2 expression in fatty liver. *Nature Communications*, 3, 672. https://doi.org/10.1038/ncomms1667

Pandey, S.K., Yu, X.X., Watts, L.M., Michael, M.D., Sloop, K.W., Rivard, A.R., Leedom, T.A., Manchem, V.P., Samadzadeh, L., McKay, R.A., Monia, B.P., Bhanot, S. (2007). Reduction of low molecular weight protein-tyrosine phosphatase expression improves hyperglycemia and insulin sensitivity in obese mice. *Journal of Biological Chemistry*, 282(19), 14291–14299. https://doi.org/10.1074/jbc.M609626200

Rieusset, J., Andreelli, F., Auboeuf, D., Roques, M., Vallier, P., Riou, J.P., Auwerx, J., Laville, M., Vidal, H. (1999). Insulin acutely regulates the expression of peroxisome proliferator-activated receptor-gamma in human adipocytes. *Diabetes*, 48(4), 699-705. https://doi.org/10.2337/diabetes.48.4.699.

Sun, C., Berry, W.L., & Olson, L.E. (2017). PDGFRalpha controls the balance of stromal and adipogenic cells during adipose tissue organogenesis. *Development*, 144(1), 83–94. https://doi.org/10.1242/dev.135962

Stanford, S.M., Aleshin, A.E., Zhang, V., Ardecky, R.J., Hedrick, M.P., Zou, J., Ganji, S. R., Bliss, M.R., Yamamoto, F., Bobkov, A.A., Kiselar, J., Liu, Y., Cadwell, G.W., Khare, S., Yu, J., Barquilla, A., Chung, T.D.Y., Mustelin, T., Schenk, S., Bankston, L.A., Liddington, R.C., Pinkerton, A.B., Bottini, N. (2017). Diabetes reversal by inhibition of the low-molecular-weight tyrosine phosphatase. *Nature Chemical Biology*, 13(6), 624–632. https://doi.org/10.1038/nchembio.2344

Stanford, S.M., Bottini, N. (2017). Targeting tyrosine phosphatases: Time to end the stigma. *Trends in Pharmacological Sciences*, 38, 524−540. https://doi.org/10.1016/j.tips.2017.03.004

Stanford, S.M., Collins, M., Diaz, M.A., Holmes, Z.J., Gries, P., Bliss, M.R., Lodi, A., Zhang, V., Tiziani, S., Bottini, N. (2021). The low molecular weight protein tyrosine phosphatase promotes adipogenesis and subcutaneous adipocyte hypertrophy. *Journal of Cellular Physiology*, 1-13. https://doi.org/10.1002/jcp.30307

Stanford, S.M., Diaz, M.A., Ardecky, R.J., Zou, J., Roosild, T., Holmes, Z.J., Nguyen, T.P., Hedrick, M.P., Rodiles, S., Guan, A., Grotegut, S., Santelli, E., Chung, T.D.Y., Jackson, M.R., Bottini, N., Pinkerton, A.B. (2021). Discovery of orally bioavailable purine-based inhibitors of the low-molecular weight protein tyrosine phosphatase. *Journal of Medicinal Chemistry*, 64, 5645-5653. https://doi.org/10.1021/acs.jmedchem.0c02126

Vaziri, C., & Faller, D.V. (1996). Down-regulation of platelet-derived growth factor receptor expression during terminal differentiation of 3T3-L1 pre-adipocyte fibroblasts. *Journal of Biological Chemistry*, 271(23), 13642–13648. https://doi.org/10.1074/jbc.271.23.13642

Wo, Y.Y., Zhou, M.M., Stevis, P., Davis, J.P., Zhang, Z.Y., Van Etten, R.L. (1992). Cloning, expression, and catalytic mechanism of the low molecular weight phosphotyrosyl protein phosphatase from bovine heart. *Biochemistry*, 31(6), 1712–1721. https://doi.org/10.1021/bi00121a019

Wu, Z., Xie, Y., Bucher, N.L., Farmer, S.R. (1995). Conditional ectopic expression of C/EBP beta in NIH-3T3 cells induces PPAR gamma and stimulates adipogenesis. *Genes & Development*, 9(19), 2350-2363, https://doi.org/10.1101/gad.9.19.2350.

Yao, C.H., Wang, R., Wang, Y., Kung, C.P., Weber, J.D., Patti, G.J. (2019). Mitochondrial fusion supports increased oxidative phosphorylation during cell proliferation. *eLife*, 8. https://doi.org/10.7554/eLife.41351

Yin, R., Dong, Y., Li, H. (2006). PPARγ phosphorylation mediated by JNK MAPK: a potential role in macrophage-derived foam cell formation. *Acta Pharmacologica Sinica*, 27(9), 1146-1152. https://doi.org/10.1111/j.1745-7254.2006.00359.x

Ying, Z., Qiang, L., & Farmer, S.R. (2006). Activation of CCAAT/enhancer-binding protein (C/EBP) alpha expression by C/EBP beta during adipogenesis requires a peroxisome proliferator-activated receptor-gamma-associated repression of HDAC1 at the C/ebp alpha gene promoter. *Journal of Biological Chemistry*, 281(12), 7960-7967, https://doi.org/10.1074/jbc.M510682200